Dynamic mechanical response of solid at high strain rate after hydrochemical corrosion

Ming Zhou[a], Lan Qiao[b], Qingwen Li[c*]

Department of Civil Engineering, University of Science and Technology Beijing, Beijing 100083, China

[a]zhoumingming12138@163.com, [b]lanqiao@ustb.edu.cn, [c*]qingwenli@ustb.edu.cn

Abstract. The underground rock mass, especially the surrounding rock of the offshore orebody, has been in the groundwater environment for a long time, and the hydrochemical corrosion has become an important factor affecting the mechanical strength of the surrounding rock. At the same time, the underground environment of "three heights and one disturbance" in the deep rock mass brings the influence of dynamic load to the surrounding rock. Therefore, it is of great significance to study the influence of hydrochemical corrosion on dynamic mechanical properties of rock to ensure the stability of surrounding rock. This paper takes granite mined from a large mine as the research object and uses the Hopkinson impact system to conduct dynamic mechanical tests on rock samples corroded by salt solutions of different concentrations plus solids. The stress-strain curve, failure form and energy evolution process of test samples are analyzed one by one. The results show that with the increase of the mass concentration of the salt solution, the impact failure strain of the specimen shows a trend of "rapidly decreasing → rapidly increasing → stable fluctuation". In addition, most of the energy entering the specimen is absorbed by the specimen for the work done by the crushing of the cement paste block and the surface energy consumed by the formation of the diameter crack of the rock block, and only a small part of the energy is transferred to the transmission rod in the form of transmission energy. As the mass concentration increases, the absorption energy consumption of the specimen decreases first and then increases, and the minimum value (about 22.32%) is obtained when the mass concentration is 10%. The conclusion can provide a theoretical basis for the dynamic impact of the offshore ore body after corrosion, which has been exposed to groundwater corrosion for a long time, and has important research significance.

Keywords: hydrochemical corrosion; dynamic mechanical strength; rock dynamics; conversion regularity

1 Introduction

The physical properties of rock materials are discontinuous and anisotropic, and the existence of groundwater has a great influence on their properties and internal cemen-

H. Bilgin et al. (eds.), *Proceedings of the 2023 5th International Conference on Civil Engineering, Environment Resources and Energy Materials (CCESEM 2023)*, Advances in Engineering Research 227,
https://doi.org/10.2991/978-94-6463-316-0_26

tation. The groundwater is rich in a variety of chemical ion components, and the rock mass is placed in a complex chemical solution environment for a long time, which is easy to react with it, and the internal structure of the rock will be rearranged, thus affecting the physical properties of the rock and the change of the internal mesostructure [1]. In recent years, the research on the mechanism of rock fracture caused by water-rock chemistry has been paid more attention by scholars at home and abroad, and fruitful research results have been obtained. Xia et al. [2] quantitatively expressed the change rule of shear strength of fracture surface with hydrochemical corrosion, and determined the optimal weakening effect of solution on fracture surface strength. Later, P. Baud et al. [3], Han et al. [4,5], Wang et al. [6], Guo et al. [7] explained the effect of chemical damage on crack growth from the perspective of fracture mechanics, and established the corresponding mechanical model. Liu[8], Chen et al. [9], Hu et al. [10], F. L. Pellet et al. [11] designed experiments related to water-rock interaction to reveal the internal mechanism of water-rock interaction from an experimental point of view. At present, researches mainly focus on the influence of water-rock chemistry on the macro-mechanical strength of intact or fractured rocks [12~15], but there are few researches on the damage mechanism of multiphase rock mass (i.e., fracture grouting plus solid) under water-rock chemistry. In addition, mineral composition, solution chemical composition, flow state and ambient temperature all have important effects on water-rock interaction [16]. Therefore, the mechanism of water-rock action in Jiaodong Peninsula should be studied in combination with the geological environment on site. At the same time, the addition of solid to the corroded rock sample is always in the underground environment of "three high and one disturbance" [17~19], and is subject to dynamic impact. Therefore, it is of important engineering practical significance to study the mechanical response of solid addition under high strain rate after hydrochemical corrosion.

In view of this, the granite core taken from the geological exploration hole of Shaling Gold Mine was processed into the standard sample of crack grouting plus solid, and after being soaked and corroded with different salt solutions, dynamic impact compression and dynamic impact splitting experiments were carried out by SHPB impact system to obtain the dynamic mechanical properties of the added solid under high strain rate after multi-salt erosion. At the same time, the internal mechanism of energy accumulation, energy dissipation, energy distribution and polysalinization damage in the progressive failure process of adding solid is analyzed from the perspective of energy.

2 Sample preparation and test plan

2.1 Test equipment and use

The dynamic uniaxial compression test adopts the traditional Hopkinson impact device. The test device is shown in Figure 1. The diameter of the pressure rod is 50 mm, its elastic modulus E is 210 GPa, the density is 7787 kg/m^3, the wave velocity is 5667 m/s, and the length of the steel rod is 1.5 m.

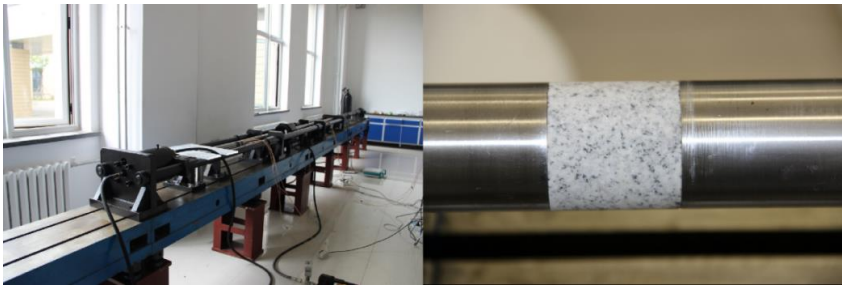

Fig. 1. Split Hopkinson pressure bar test device

For the impact splitting test, the impact bullet was selected as a spindle bullet, the impact pressure was 0.5MPa and remained constant, and the fissure filling of the specimen should be parallel to the end face of the pressure rod. The test specimen and pressure rod are shown in Figure 2.

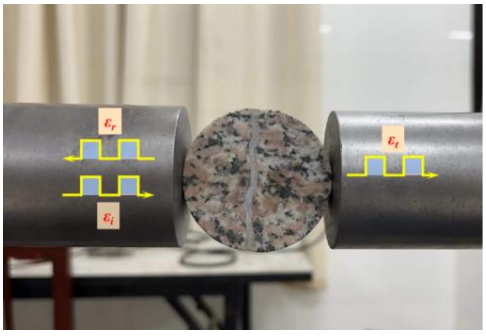

Fig. 2. Diagram of orientation of crack grouting material and shock wave

2.2 Sample preparation

The preparation process of grouting disc with fissure used in SHPB test and the treatment plan of salt solution immersion are as follows: (1) The standard Brazilian disc sample Φ50mm×25mm was prepared by drilling core and grinding technology; (2) Natural joint cracks were prepared by Brazil disc static splitting method; (3) The crack width is controlled to 2mm, and cement slurry is injected into the crack spacing; (4) After the cement slurry solidifies, remove the mold, and place the specimen in clean water for 24h; (5) Samples were taken out and placed in composite salt solution with mass concentration of 5%, 10%, 15% and 20%, and soaked for 30d, 60d, 90d and 120d, respectively. The preparation process of the Brazilian disk sample with crack grouting is shown in Figure 3.

Fig. 3. Preparation process of grouting rock sample used in the test

3 Analysis of dynamic characteristics and test results

3.1 Dynamic compressive strength, tensile strength and test crushing energy consumption

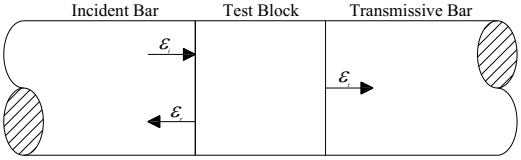

Fig. 4. Schematic diagram of SHPB impact compression test loading

The stress, strain and strain rate of the impact rock can be obtained by using the three-wave formula because the conventional dynamic compressive test satisfies the one-dimensional stress state and the assumption of stress-strain uniformity.As shown in Figure 4.

At the same time, we can obtain the incident energy, reflected energy, transmitted energy and crushing absorption energy of rocks in the process of impact compression and failure through the energy formula, as shown in equations (1)~ equations(4).

$$W_i = \frac{A_0 C_0}{E} \int \sigma_i^2 dt = A_0 C_0 E \int_0^t \varepsilon_i^2 dt \sigma_t \tag{1}$$

$$W_r = \frac{A_0 C_0}{E} \int \sigma_r^2 dt = A_0 C_0 E \int_0^t \varepsilon_r^2 dt \tag{2}$$

$$W_t = \frac{A_0 C_0}{E} \int \sigma_t^2 dt = A_0 C_0 E \int_0^t \varepsilon_t^2 dt \tag{3}$$

$$W_a = W_i - W_r - W_t \tag{4}$$

where, A_s is the cross-sectional area of the test block; l_s is the initial length of the test block; A_0 is the cross-sectional area of the bar; C_0 Is the propagation velocity of stress wave in the bar; E is the elastic modulus of the pressure bar; σ_i, ε_i is the stress and strain of the incident bar; σ_r, ε_r is the stress and strain of the reflecting bar; σ_t, ε_t is the stress and strain of the transmission bar; W_i is the incident energy; W_r is the reflection energy; W_t is the transmission energy; W_a is the energy consumption of the broken.

For dynamic splitting test, the loading diagram of SHPB Brazil splitting test is shown in Figure 5. Suppose that the diameter of the Brazilian disk is D, the thickness is B, A is any point on the line between the two contact force points, and the distance between the two contact force points and point A is r_1 and r_2, respectively, then $r_1 + r_2 = D$.

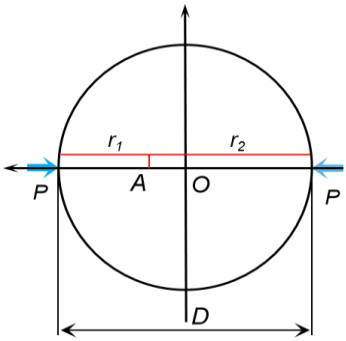

Fig. 5. SHPB Brazil splitting test loading diagram

According to elastic mechanics, the principle state of the compression diameter of the center is:

$$\varepsilon(t) = \frac{C_0}{D} \int_0^t \left[\varepsilon_i(t) - \varepsilon_r(t) - \varepsilon_t(t) \right] dt \tag{5}$$

$$\begin{cases} \sigma_x = -\dfrac{2P}{\pi DB} \\ \sigma_y = \dfrac{2P}{\pi B}\left(\dfrac{1}{r_1} + \dfrac{1}{r_2}\right) - \dfrac{2P}{\pi DB} \end{cases} \tag{6}$$

We can finally determine the dynamic tensile stress of the specimen as follows:

$$\sigma_t = \frac{2E_0 A_0 \varepsilon_t(t)}{\pi DB} \tag{7}$$

3.2 Stress balance analysis

Figure 6 shows the equilibrium state of impact and waveform of specimens under different immersion concentrations.

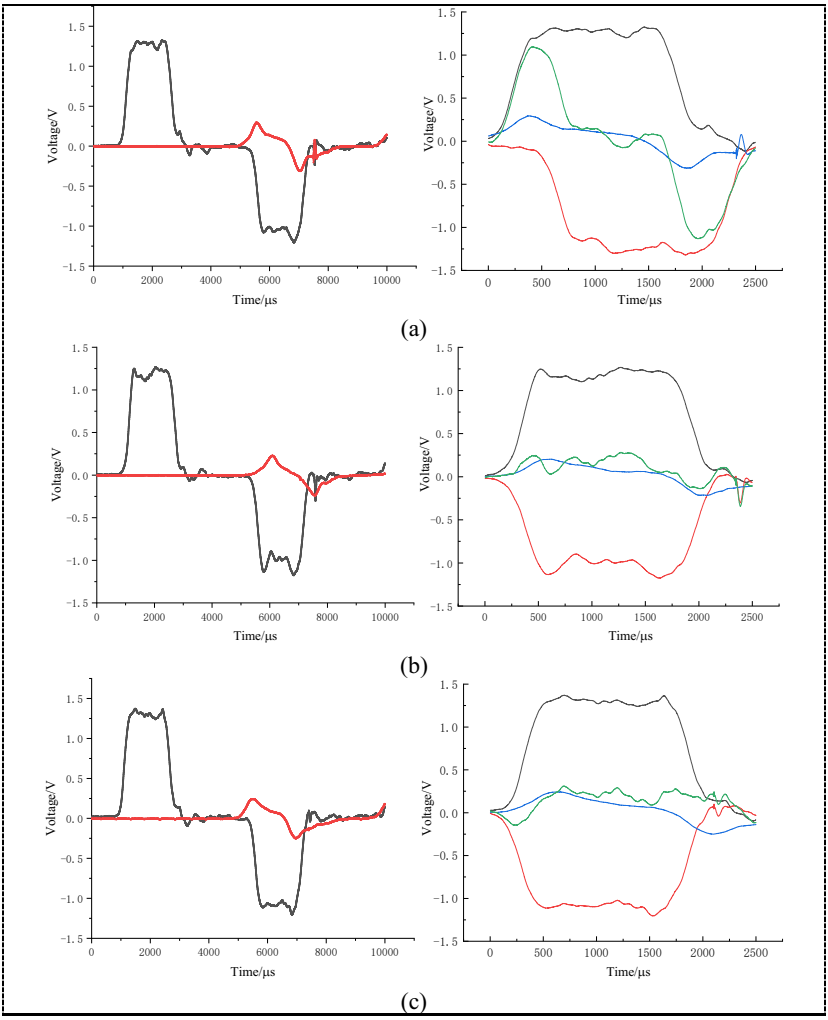

Fig. 6. Impact waveform and force balance under different immersion solution concentrations (T=30d): (a)5%-1, (b)10%-2, (c)15%-1

It can be seen from the figure that the sum of the incident wave and reflected wave is similar to the shape evolution and voltage value of the transmitted wave, indicating that the stress waves at both ends of the specimen meet the stress equilibrium condition, that is, the rationality of using the three-wave formula to calculate the stress, strain and energy of the specimen. In the test, due to the abnormal reflected wave data of specimens 60, 90 and 120d, further noise reduction and wave cancellation processing are required. Therefore, the paper focuses on analyzing the data of specimens soaked 0 and 30d to explore the influence of solution concentration on the tensile properties of the added solid.

3.3 Stress-strain curve analysis

According to equations (5) and equations (6), the stress-strain curve of the specimen under the impact pressure of 0.5MPa after soaking for 30d with different mass concentrations is shown in Figure 7. As can be seen from the figure, stress-strain curves of specimens before and after immersion in salt solution show certain differences after the peak strength. For example, for specimens that have not been treated with salt solution, the stress drops rapidly after the peak strength to form a stress horizontal platform, while the length of the post-peak stress horizontal platform gradually decreases with the increase of the mass concentration of salt solution, and the mass concentration of 5% is the transition point of this change. Both types of curves are shown in Figure 7 (b). The gradual shortening of the stress horizontal platform makes the post-peak stress drop of the specimen gradually change from a sharp drop to a slow drop, which provides a certain adjustment time for the internal stress redistribution of the specimen, and shows that the crack propagation and diffusion rate slows down on a macroscopic level. In other words, under the action of hydrochemical erosion of salt solution, the energy released per unit time during the failure of the specimen decreases.

The dynamic tensile strength and failure strain of specimens under various working conditions as shown in Figure 7 are extracted, as shown in Figure 8. It can be seen from the figure that with the increase of salt solution concentration, the failure strain of the specimen presents a changing trend of "rapidly decreasing → rapidly increasing → tending to stable fluctuation". It can be seen that in a short period of time, the deformation capacity of the specimen is reduced by low concentration, while the failure limit of time deformation is increased by high concentration.

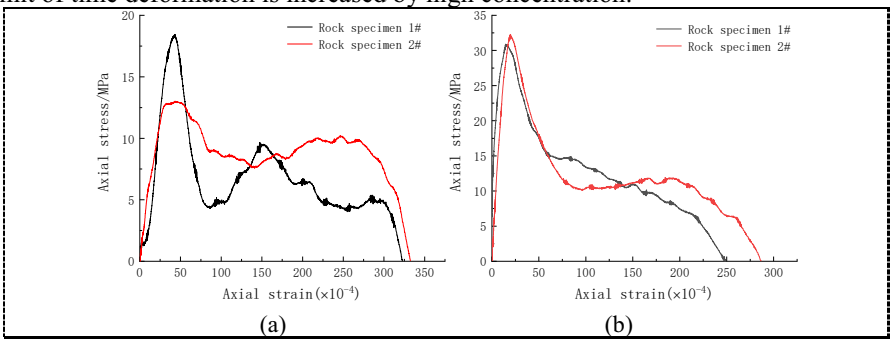

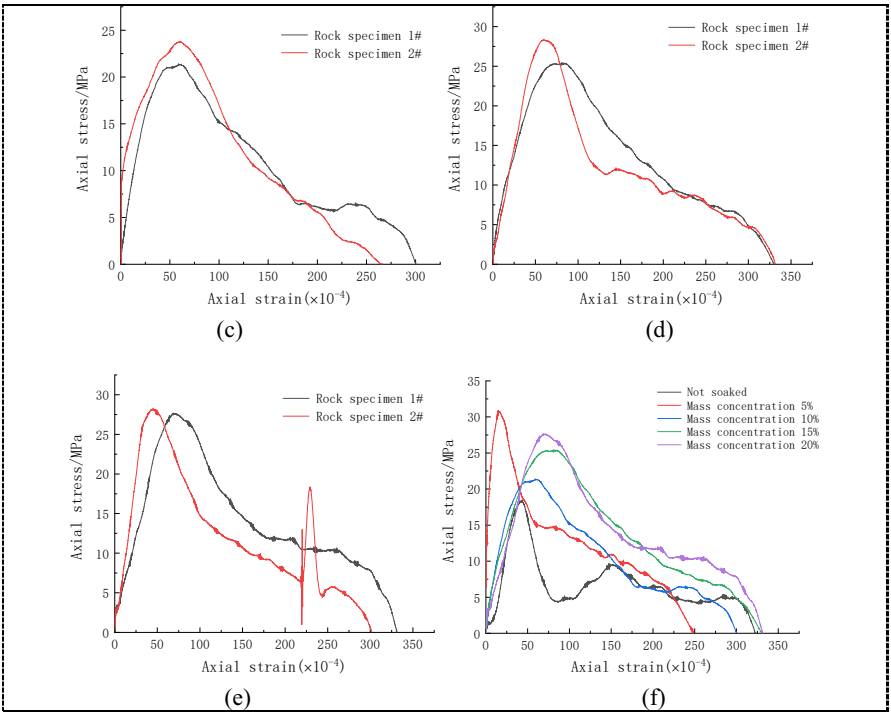

Fig. 7. Stress-strain curves of specimens soaked in salt solutions of different concentrations (T=30d): (a)unsoaked, (b)5%, (c)10%, (d)15%, (e)20%, (f)data summary

The peak strength shows a trend of "rapid increase → rapid decrease → stable fluctuation". It can be seen that under the short-term soaking time (30d), the salt solution has a positive effect on the corrosion products formed by adding solids, which is microcosm related to the filling of pores by corrosion products. In addition, with the increase of concentration, the strength showed a change of "rapidly decreasing → stable fluctuation". This is because when the solution concentration was high, the surface of the specimen reacted violently with the solution, and its pores were easy to be filled by corrosion products, thus blocking the diffusion depth of the salt solution. Therefore, the maximum value of 31.5MPa was obtained when the concentration was 5%. However, with the increase of water-rock interaction time, corrosion products gradually accumulate in the pores to form crystalline pressure, which will expand the primary pores and aggravate the damage, thus forming a "positive and negative effect" cyclic damage.

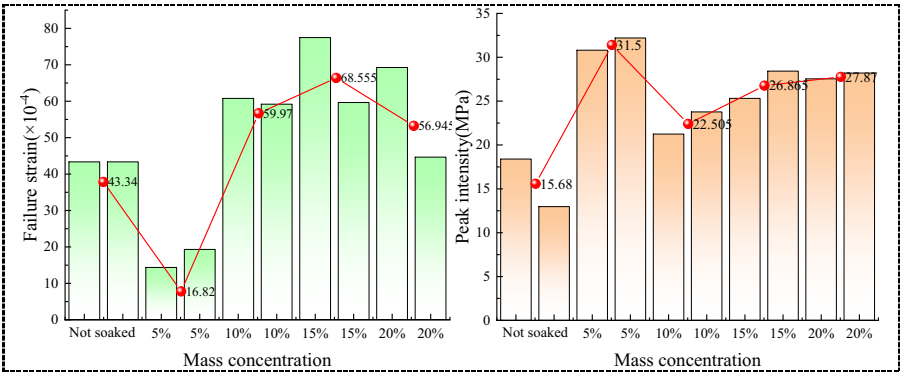

Fig. 8. Dynamic tensile strength and failure strain of specimens under various working conditions

3.4 Analysis of energy evolution

According to equations (1)~equations (4), the energy evolution curve with time during the dynamic tensile process of the specimen can be obtained. Figure 9 shows the internal energy transformation of the specimen under the impact pressure of 0.5MPa. It can be seen from the figure that the incident energy, reflected energy and absorbed energy of the specimen increase with the increase of the impact load acting time, and remain constant after reaching a certain value, while the increase amplitude of the transmitted energy of the specimen is obviously small under the same order of magnitude, showing a continuous and slow increase. It is assumed that the specimen meets the energy conservation in dynamic tensile failure, and the energy reflection loss is negligible at the contact interface between the compression rod and the specimen. Since the specimen is in contact with the approximate contact line of the pressure bar, most of the incident energy is reflected back into the incident bar at the contact interface between the pressure bar and the specimen. As shown in Figure 9 (f), the ratio of reflected energy to incident energy of the specimen is more than 70%, the ratio of absorbed energy to total energy is about 20%-40%, and the ratio of transmitted energy to total energy is about 2%. Among them, most of the energy entering the specimen is absorbed by the specimen for the work done by the crushing of the cement paste block and the surface energy consumed by the formation of the diametral crack of the rock block, and only a small part of the energy is transferred to the transmission rod in the form of transmission energy.

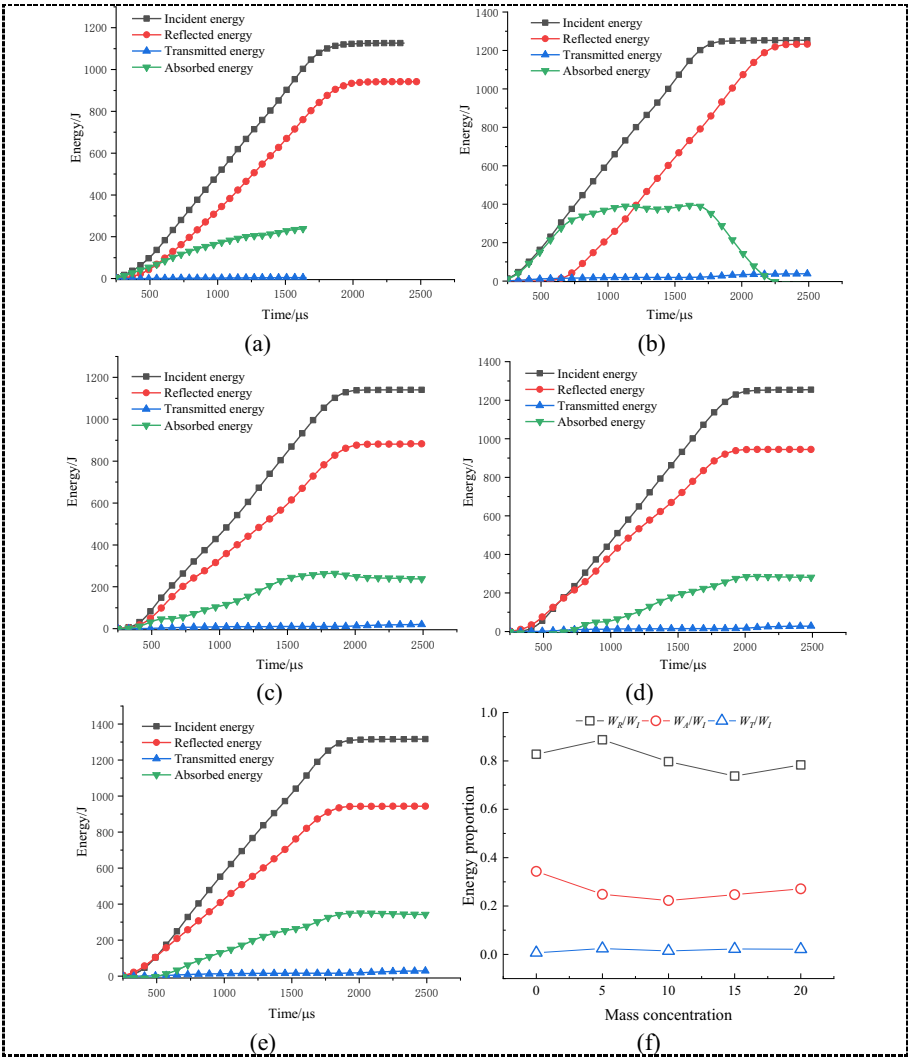

Fig. 9. Energy evolution curve of specimens under different soaking concentrations: (a)unsoaked, (b)5%, (c)10%, (d)15%, (e)20%, (f)energy proportion

4 Discussion

(1) Under a certain confining pressure, with the increase of salt solution soaking time, the concave of the compaction section and the convex of the yield section become more significant before the peak. The peak strength is also lower, but the corresponding strain increases. With the increase of salt solution concentration after peak, the stress drop rate of the sample is slower, and the stress plateau of the residual section is more obvious. The maximum total input energy of the specimen decreases greatly at

the 60d, and changes and fluctuations are relatively stable after 60d. According to Figure. 9 (f), it can be observed that the change of elastic energy limit is more sensitive to the concentration of soaking solution than the change of soaking time.

(2) Figure 10 shows the relationship between the absorption energy proportion of the specimen and the solution concentration. It can be seen from the figure that the proportion of absorbed energy (about 34.34%) of the specimen without solution treatment is significantly higher than that of the specimen soaked in salt solution, reflecting that the energy absorbed by the failure of the solid after being eroded by salt solution is reduced. It can also be seen from the figure that with the increase of mass concentration, the absorption energy of the specimen first decreases and then increases, and the minimum value is obtained when the mass concentration is 10% (about 22.32%), indicating that the erosion mechanism of the salt solution on the specimen, the erosion time and the solution concentration are not simply superimposed by a single factor, but interact with each other.

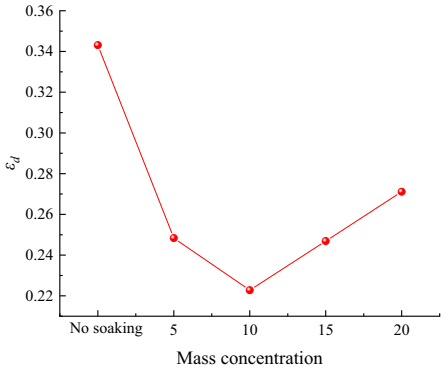

Fig. 10. The relationship between absorption energy proportion and solution concentration

5 Conclusion

(1) With the increase of the mass concentration of the salt solution, the impact failure strain of the specimen presents a change of "rapidly decreasing → rapidly increasing → tending to stable fluctuation". It can be seen that the deformation capacity of the specimen is reduced at low concentration in a short time, while the time deformation failure limit is increased at high concentration.

(2) With the increase of the mass concentration of the salt solution, the peak impact failure strength of the specimen presents a change of "rapidly increasing → rapidly decreasing → stable fluctuation". It can be seen that under the short-term soaking time (30d), the salt solution has a positive effect on the corrosion products formed by adding solid, which is microcosm related to the filling pores of the corrosion products

(3) The ratio of reflected energy to incident energy is more than 70%, the ratio of absorbed energy to total energy is about 20%~40%, and the ratio of transmitted energy to total energy is about 2%. That is, most of the energy entering the specimen is

absorbed by the specimen for the work done by the crushing of the cement paste block and the surface energy consumed by the formation of the diametral crack of the rock block, and only a small part of the energy is transferred to the transmission rod in the form of transmission energy

(4) With the increase of solution concentration, the absorbed energy consumption of the specimen first decreased and then increased, and the minimum value (about 22.32%) was obtained when the mass concentration was 10%, indicating that the erosion mechanism of the salt solution on the specimen, the erosion time and solution concentration were not simply superimposed by a single factor, but influenced by each other.

Acknowledgments

This research was funded by the National Natural Science Foundation of China, grantnumber 52274107 and Interdisciplinary Research Project for Young Teachers of USTB (FRF-IDRY-GD21-001).

References

1. Zheng J , Yang J , Xi Z . 2014 J.Influence of pore structures on the mechanical behavior of low-permeability sandstones: numerical reconstruction and analysis. International Journal of Coal Science & Technology, 1(003):329-337.
2. Xia B W , Xu M X , Pan C . 2019 J. Mechanical Properties of the Hard Sandstone Fracture Surface under Hydrochemical Corrosion . Journal of Engineering, 6:1-11.
3. Baud P , Zhu W , Wong T F . 2000 J. Failure mode and weakening effect of water on sandstone. Journal of Geophysical Research Solid Earth, 105(B7):16371-16389.
4. Han T , Shi J , Chen Y ,et al. 2018 J. Quantifying Microstructural Damage of Sandstone after Hydrochemical Corrosion . International Journal of Geomechanics, 18(10):04018121.1-04018121.13.
5. Han T , Chen Y , Shi J ,et al. 2014 J. Experimental Study of the Influence of Hydrochemical Corrosion on Mechanical Characteristics of Concrete Materials . Journal of Experimental Mechanics, 29(06):785-793.
6. Wang Y X , Cao P . 2009 J. Study on Mechanical Damage Effect for Rock Under Hydrochemical Erosion . Journal of University of South China(Science and Technology), 23(01):27-30.
7. Cai Y Y , Yu J , Fu G F ,et al. 2016 J. Experimental investigation on the relevance of mechanical properties and porosity of sandstone after hydrochemical erosion . Journal of Mountain Science, 13(11):2053-2068.
8. Liu Y , Yang G , Wang J X ,et al. 2018 J. Fatigue deformation characteristics of limestone under the combined action of hydrochemical solution and cyclic loading . Journal of Dalian Maritime University, 2018.
9. Chen W ,J Liu J , Peng W Q , et al. 2023 J. Aging deterioration of mechanical properties on coal-rock combinations considering hydro-chemical corrosion . Energy,2023,282.
10. Hu J C , et al. 2022 J. Experimental Study on Creep of Sandstone under Hydrochemical Corrosion. Journal of Physics: Conference Series,2148(1).

11. Pellet F L , Keshavarz M , Boulon M . 2013 J. Influence of humidity conditions on shear strength of clay rock discontinuities . Engineering Geology, 157:33-38.
12. Bo S,Xingyue L,Kai C, et al. 2023 J. Experimental study on the effects of hydrochemistry and periodic changes in temperature and humidity on sandstone weathering in the Longshan Grottoes. Heritage Science,11(1).
13. Pan J L , Cai M F , Li P , et al. 2022 J. Adamage constitutive model of rock-like materials containing a single crack under the action of chemical corrosion and uniaxial compression . Journal of Central South University,29(02):486-498.
14. Yu J , Zhang X , Cai Y Y , et al. 2019 J. Meso-damage and mechanical properties degradation of sandstone under combined effect of water chemical corrosion and freeze-thaw cycles . Rock and Soil Mechanics,40(02):455-464.
15. Wu Y L., Dong Q Q , He J . 2021 J. The Effect of Chemical Corrosion on Mechanics and Failure Behaviour of Limestone Containing a Single Kinked Fissure. Sensors,21(16).
16. Koji, Masuda. . 2001 J. Effects of water on rock strength in a brittle regime. Journal of Structural Geology, 2001.
17. Tobias L . 2023 J. Considerations Related to Active Stress Management in Deep Mining. BHM Berg- und Hüttenmännische Monatshefte,168(10).
18. He M C . 2006 J. Rock mechanics and hazard control in deep mining engineering in china. 2006.DOI:10.1142/9789812772411_0003.
19. Qian Q H . 2004 J. The Characteristic Scientific Phenomena of Engineering Response to Deep Rock Mass and the Implication of Deepness.Journal of East China Institute of Technology 2004(01):1-5.